
Improvement of X-Ray Diffraction Geometries of Water Physisorbed in Zeolites on the Basis of Periodic Hartree–Fock Calculations

A. V. LARIN,^{1,2} D. N. TRUBNIKOV,² D. P. VERCAUTEREN¹

¹Laboratoire de Physico-Chimie Informatique, Facultés Universitaires Notre Dame de la Paix (FUNDP), Rue de Bruxelles 61, B-5000 Namur, Belgium

²Department of Chemistry, Moscow State University, Leninskie Gory, Moscow, B-234, 119899, Russia

Received 24 September 2004; accepted 4 October 2004

Published online 14 January 2005 in Wiley InterScience (www.interscience.wiley.com).

DOI 10.1002/qua.20463

ABSTRACT: Improvements to the experimental X-ray diffraction (XRD) coordinates of water adsorbed in three cationic zeolites as well as to the coordinates of the framework atoms is suggested on the basis of periodic DFT (PDFT) and Hartree–Fock (PHF) calculations. After an initial optimization of either the water coordinates solely or the water/zeolite framework coordinates with the minimal STO-3G basis set, a scaling procedure is proposed to improve the water O–H bond lengths and H–O–H angle up to a higher quality basis set level. It is followed by a discussion on the similarity of the hydrogen bond characteristics between water clusters and the adsorbed state.

© 2005 Wiley Periodicals, Inc. Int J Quantum Chem 102: 971–979, 2005

Key words: periodic DFT; periodic Hartree–Fock; water; aluminosilicate; hydrogen bond

Introduction

The possibility to optimize the 3D periodic structures of various series of crystalline materials considering periodic DFT (PDFT) and periodic Hartree–Fock (PHF) with different basis sets

has been demonstrated relatively recently [1–6]. However, when optimizing systems like large size zeolites, i.e., with a large number of atoms per elementary unit cell, with and/or without adsorbed molecules, only the minimal STO-3G basis set, with few exceptions, has been shown to be applicable so far. In these cases, the obtained optimized framework geometries were, for example, validated by comparison between the experimental quadrupole coupling constants and the calculated $C_{\text{qq}}(^2\text{H})$ val-

Correspondence to: D. P. Vercauteren; e-mail: daniel.vercauteren@fundp.ac.be

ues for the O—H bridge moieties of H-form aluminosilicates, or the calculated $C_{\text{qq}}(^{17}\text{O})$ and $C_{\text{qq}}(^{27}\text{Al})$ values in H-form and cationic aluminosilicates [2, 4].

To the contrary, in the case of H_2O adsorbed in several cationic form zeolites, it has been shown that the STO-3G basis could lead to O—H bond lengths elongated up to 0.99–1.01 Å as compared to those, i.e., around 0.96 Å, obtained at the higher MP2/6-311+G** level for ion-water clusters [6]. Moreover, despite a reasonable H—O—H valence angle, as well as a logical water oxygen–framework cation distance obtained by PHF/STO-3G optimization, single geometry point computations at a high basis set level such as PHF/6-21G* did not corroborate the most favored optimized PHF/STO-3G geometry of the considered water/zeolite systems [5, 6].

Comparing the H_2O geometries obtained in Refs. [5, 6] to the ones obtained with ab initio molecular dynamics (AIMD) based on the Becke exchange and Perdew correlation functionals [7], it should be noted that in the last reference, the O—H distances were overestimated, 0.989 Å for $\text{H}_2\text{O}/\text{LiABW}$ or 0.993 Å for $\text{H}_2\text{O}/\text{LiBIK}$, which is usual with DFT, and that no differences between the water O—H bond lengths depending on the hydrogen bonds (HBs) with the framework were observed [7]. However, clear O—H variations with hydrogen bonding were proven for a series of $(\text{H}_2\text{O})_n$ clusters at both the HF ($n = 2\text{--}6$) and MP2 ($n = 2\text{--}4$) levels with the aug-cc-pVDZ basis set level [8]. More precisely, there is thus a correlation between the valence $\text{O}_w\text{—H}$ and hydrogen $\text{O}'_w \dots \text{H}$ bonds when H_2O is hydrogen bonded. The HB distances in H_2O clusters range from 1.76 in cyclic pentamers to 1.9 Å in dimers resulting in $\text{O}_w\text{—H}$ variations from 0.02 to 0.007 Å, respectively, at the MP2/aug-cc-pVDZ level [8]. Thus, as soon as all known experimental examples of $\text{H}_2\text{O}/\text{zeolite}$ systems correspond to $\text{O}_w \dots \text{H}$ values of 1.866 Å and higher [9–11], this lower $\text{O}_w \dots \text{H}$ value together with the $\text{O}_w\text{—H}$ increase predicted theoretically for the HB water proton by analogy with H_2O clusters [8] allows to suggest an O—H elongation in the adsorbed state of 0.01 Å at most. The equal $\text{O}_w\text{—H}_1$ and $\text{O}_w\text{—H}_2$ bond lengths of 0.989 Å and the absence of any $\text{O}_w\text{—H}/\text{O}'_w \dots \text{H}$ correlation in [7] taking into account a strong difference in the HB lengths of 1.866 and 2.265 Å related to each of the H_2O protons in LiBIK are in a contradiction with the results of Refs. [6, 8].

In this work, we thus wish to elucidate the extent of the O—H distortions of H_2O adsorbed in several

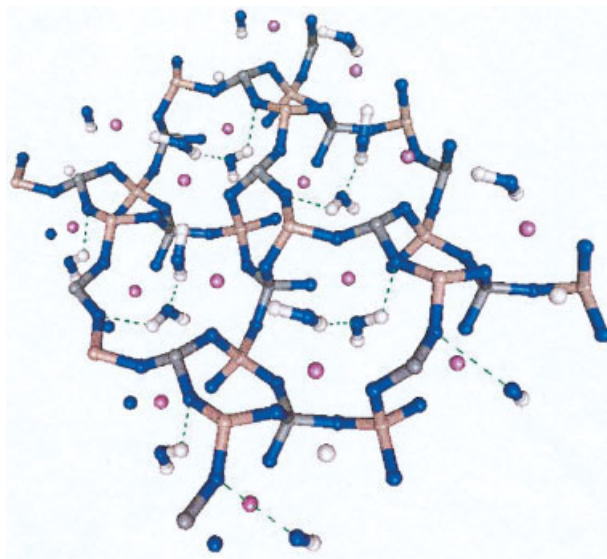


FIGURE 1. Three-dimensional structure of the LiABW zeolite including adsorbed water [9]. Hydrogen bonds are shown by dashed lines. [Color figure can be viewed in the online issue, which is available at www.interscience.wiley.com.]

chosen zeolite models, and consequently improve the available XRD data. Particularly, we proposed a three-step optimization procedure: (1) an initial PHF optimization of the water geometry together with a part of the zeolite with the minimal STO-3G basis set followed by (2) a distance (s) and angle (t) scaling of the “isolated whole H_2O molecule” to an upper level of theory and basis sets (conserving the ratios of O—H lengths obtained at the first step), and (3) an optimization of the proton positions in the $\text{H}_2\text{O}/\text{zeolite}$ via systematic variations of each O—H bond length and of the H—O—H angles. The improved coordinates of the H_2O atoms as well as of the zeolite framework atoms (when optimized) will be discussed.

Zeolite Models and Computational Details

The optimizations of the LiABW [9] (Fig. 1), NaNAT [10] (Fig. 2), and BaEDI [11] (Fig. 3) hydrated structures (Table I) were carried out at the STO-3G level for the framework atoms and 6-1G, 8-511G, and pseudopotential Hay–Wadt (small core or HWSC [12]) level for the Li, Na, and Ba cations, respectively, using both the PHF and PDFT CRYSTAL95 code [12], in which we adopted the Polak–

Ribiere algorithm. For NaNAT, the coordinates of both the cations and the H₂O atoms were optimized, whereas for BaEDI only the H₂O atomic coordinates were optimized. For LiABW, the procedure also included the optimization of the cell parameters, the coordinates of Li and the ones of the O₂, O₃, and O₄ atoms, i.e., the three framework atoms closest to Li. For comparison of the HB characteristics, we also performed geometry optimizations of the isolated H₂O molecule and of Me⁺(H₂O) clusters (Me = Li and Na) using Gaussian98 [13].

To calculate the electronic properties with high level basis sets, single-point calculations for all three systems were performed with the pseudopotential (ps) Durant–Barthelat basis with d polarization functions for Si and Al, with the 6-1G*, 8-511G*, and HWSC plus polarization basis sets for Li, Na, and Ba, respectively, and 6-21G** for H and O. The used sp/d exponents were 0.9, 0.12339/0.5, 0.17/0.45, and 0.3737/0.6 au⁻² on the H, Al, Si, and O atoms, respectively. The d exponents on Li, Na, and Ba were 0.8, 0.175, and 0.33 au⁻², respectively.

To additionally verify the validity of the optimized LiABW zeolite model obtained at the 6-21G** level, a full electron 8-511G*(Al)/8-411G*(O)/66-21G*(Si)/21G*(H) basis set, whose sp/d exponents were varied as compared to those in Ref. [12], was

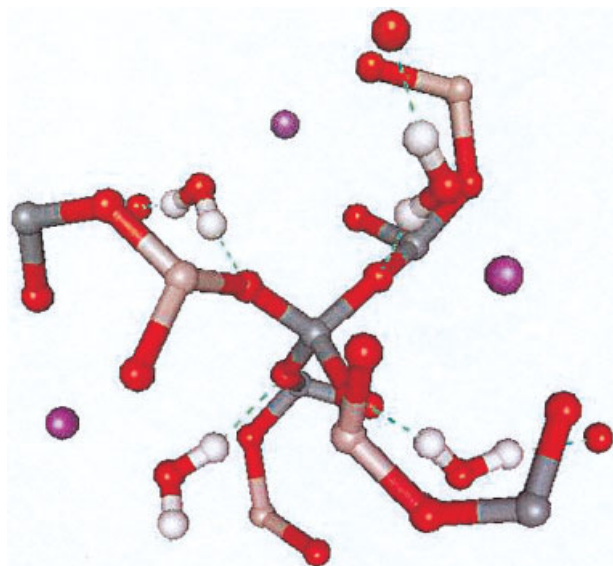


FIGURE 2. Three-dimensional structure of the NaNAT zeolite including adsorbed water [10]. Hydrogen bonds are shown by dashed lines. [Color figure can be viewed in the online issue, which is available at www.interscience.wiley.com.]

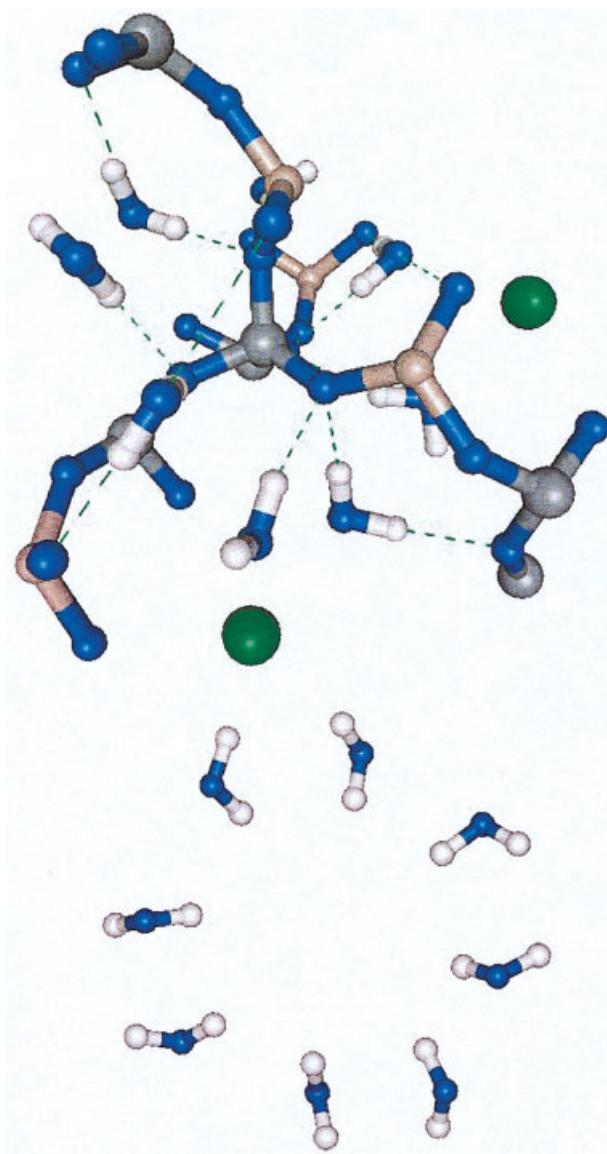


FIGURE 3. Three-dimensional structure of the BaEDI zeolite including adsorbed water [11] (top) and particular 8-ring water “cluster” within the BaEDI structure (bottom). Hydrogen bonds are shown by dashed lines. [Color figure can be viewed in the online issue, which is available at www.interscience.wiley.com.]

also applied. Finally, DFT calculations were also performed with the hybrid Perdew–Burke–Ernzerhof (PBE) functional for both exchange and correlation terms (including a 30% of Hartree–Fock correlation term) and B3LYP with the pseudopotential Durant–Barthelat basis described above. All computations with CRYSTAL95 and Gaussian98 were carried out on an IBM 15-node (120-MHz) Scalable

TABLE I

Symbol, number of atoms, and water molecules, of different Al, Si, and O types of atomic orbitals (AO) per elementary unit cell (UC), and symmetry group of the three cationic zeolites.

Name	Symbol	Atoms/UC ^a	H ₂ O/UC	n _{Al} /n _{Si} /n _O	AO/UC ^b	Symmetry
LiABW	LiABW	28/40	4	1/1/4	464/584	Pna2 ₁
Natrolite	NaNAT	34/46	4	1/2/5	578/724	Fdd2
Edingtonite	BaEDI	32/56	8	1/2/5	628/790	P2 ₁ 2 ₁ 2

^a For dehydrated/hydrated forms.

^b Hydrated form at the ps-21G** or 8-511G*(Al)/8-411G*(O)/66-21G*(Si)/21G*(H) levels.

POWERparallel platform (1 Gb of memory/CPU) with conventional tolerance criterions (10^{-5} , 10^{-5} , 10^{-5} , 10^{-7} , 10^{-10}) for the bielectronic integrals.

Before discussing the optimized theoretical geometries, one should remember that the relative H₂O locations as determined by XRD are totally different in all three zeolites. The main differences between the cyclic H₂O "cluster" in BaEDI and the linear chains in LiABW (Fig. 1) are the presence of weak O_w...H HBs around 2.3 Å in the H₂O chain and a negligible HB influence on the H₂O ring with the shortest O...H distance of 2.657 Å (Fig. 3). Water molecules in NaNAT participate in ...-(Na⁺-H₂O)_n-... chains with Na-O_w distances of 2.345 and 2.382 Å without direct HBs between the H₂O molecules (Fig. 2) [10].

Results and Discussion

Detailed discussions on the STO-3G theoretically optimized zeolite cationic models can be found elsewhere [5, 6]. The H₂O geometries optimized with or without part of the zeolite framework (lines denoted as "PHF/basis(Me)/basis(Si, Al, O, H)" in Table II) possess smaller H₁-O-H₂ angles, and closer H₁-O and O-H₂ distances (H₁ and H₂ belonging to the same molecule) as compared to the initial XRD models. Their localizations in the framework can be evaluated by looking to the distances between the water O atom and the respective zeolite Me cation. Me-O_w distances are close to the sum of the van der Waals (vdW) radius of the Me ion and O atom for Na-O_w and Ba-O_w in NaNAT and BaEDI, respectively. For LiABW, the calculated Li-O_w distances are slightly smaller than the sum of the vdW radius.

After a PHF optimization of the H₂O/zeolite systems with the STO-3G basis, single geometry point PHF calculations were realized at the higher

ps-21G** level. The latter showed a higher energy (i.e., less stable) as compared to the XRD initial structures (Table III, case with scaling factor $s = 1.0$, positive values), with the exception of the LiABW case.

As we noted in the Introduction, rather large O-H differences in physisorbed H₂O molecules were obtained by optimization of the water/zeolite systems at the STO-3G level: 0.02 Å for an HB length around 2.2 Å in H₂O/LiABW (Table IV), comparable to the strong O-H elongation of 0.02 Å, which was shown to appear at shorter HB length of 1.76 Å in (H₂O)₅ cluster [8]. To "compensate" the excessive distortions with STO-3G, we scaled the H₂O geometry only. The H₂O molecules can indeed be tackled as a relatively independent adsorbate subsystem as shown by comparison of the measured and calculated quadrupole coupling constants C_{qq} of the ²H and ¹⁷O nuclei of the adsorbed H₂O molecules; their values are much closer to the gas state than to those in the liquid or crystal phases [6].

The H₂O parameters optimized with Gaussian98 at the HF/STO-3G, HF/6-21G**, and B3LYP/6-21G** levels are: H-O-H = 100°1, 103°7, and 101°1, |O-H| = 0.989, 0.949, and 0.975 Å, respectively. The obtained HF/6-21G** geometry is close to the one observed experimentally in the gas state: H-O-H = 103°9 and |O-H| = 0.959 Å [14], whereas the B3LYP/6-21G** results are far from the experimental ones. The ratio of the water O-H bond lengths, $s = |\text{O-H}|_{\text{STO-3G}}/|\text{O-H}|_{6-21\text{G}^{**}}$, and H-O-H angles, $t = \text{H-O-H}|_{\text{STO-3G}}/|\text{H-O-H}|_{6-21\text{G}^{**}}$ for H₂O in the gas state, allowed us to determine two scaling factors at the HF level: $s = 1.0422$ and $t = 0.9648$. Respective B3LYP scaling factors are $s = 1.014$ and $t = 0.997$. Because the optimal s and t values, i.e., those that lead to the minimum of the total water/zeolite energy, cannot necessarily coincide with the one determined above

TABLE II

Water geometries and water oxygen-metal ion distances, Me—O (Me = Li, Na, and Ba), for the three cationic zeolites: experimental data (XRD), ab initio molecular dynamics (AIMD) with Becke exchange and Perdew correlation functionals for LiABW [7], and models optimized with CRYSTAL through periodic HF (PHF) and scaled with periodic DFT (PDFT).

Zeolite	Method	Me—O, Å ^a	R _{OH} , Å	H—O—H, °
LiABW	XRD [9]	1.913, 1.968w, 1.981, 1.942	0.955, 1.096	126.4
	AIMD [7]	—	2 × 0.989	106.8
	PHF/6-1G/STO-3G ^b	1.814w, 1.878, 2 × 1.942	1.012, 0.993	105.4
	PDFT/scaling	“	0.979, 0.973	108.2
NaNAT	XRD [10]	2.367, 2.370w, 2.391w, 2.395, 2.518	0.974, 0.968	114.0
	PHF/8-511G/STO-3G ^c	2.345w, 2.368, 2.380, 2.382w, 2.512	1.003, 0.995	109.2
	PDFT/scaling	“	0.982, 0.972	107.6
BaEDI	XRD [11]	2 × 2.792w, 2 × 2.788w	0.959, 0.928, 0.942, 0.956	101.7, 111.3
	PHF/HWSC/STO-3G ^d	2 × 2.729w, 2 × 2.746w	0.993, 0.994, 0.993, 0.995	100.9, 104.1
	PDFT/scaling	“	0.978, 0.973, 0.972, 0.972	101.7, 105.8
	Exper. (gas phase) [14]	—	0.959	103.9

Basis sets for the optimization are denoted first for the Me ion and then for Al, Si, O, H atoms. Bold notations refer to the final water geometry obtained with O—H and H—O—H scaling.

^a Denotes distance to H₂O oxygens, others refer to zeolite oxygens.

^b PHF optimization of all cell sizes and Li⁺, O₂, O₃, and O₄ atomic coordinates.

^c PHF optimizations of Na⁺ and H₂O coordinates only.

^d PHF optimization of H₂O coordinates.

TABLE III

Total energy variation (kcal/mol) of the PHF optimized cationic water/zeolite models relative to the energy of the initial XRD models with respect to the scaling factor *s* for the O—H bond length of water (zero energy for each model corresponds to the respective XRD structure).

Zeolite	<i>s</i>					
	1.0	1.02	1.0352	1.0422	1.05	1.07
LiABW/PHF	-54.7	-61.6	-64.7	-65.5	-65.9	-64.6
LiABW/PDFT	-45.0	-47.7	-48.3	-47.8	-46.9	—
LiABW/PHF*	—	—	—	-61.0	-62.2	-63.1
LiABW/PDFT*	—	—	-49.4	-49.7	-49.6	-47.2
NaNAT/PHF	3.8	2.0	-2.8	-4.45	-4.53	-2.0
NaNAT/PDFT	-2.5	-4.2	-3.9	-2.5	-1.3	—
BaEDI/PHF	14.1	2.9	-1.2	-1.6	-1.1	—
BaEDI/PDFT	-6.1	-9.8	-8.3	-6.4	-3.2	—

The scaling is applied after PHF optimization at fixed positions of the water oxygen atoms. The pseudopotential HWSC*(Ba), full electron 8-51G*(Na), and 6-1G*(Li) basis sets were used for the cations. PHF and PDFT with Perdew–Burke–Ernzerhof hybrid functional (30 % of HF exchange) results were considered with the pseudopotential ps-21G*(Al, Si)/6-21G*(O, H) basis set for NaNAT and BaEDI and the pseudopotential ps-21G*(Al, Si)/6-21G*(O, H) or full electron (denoted by *) 8-511G*(Al)/66-21G*(Si)/8-411G*(O)/6-21G*(H) basis sets [14] for LiABW. Bold notations refer to energy minimum.

TABLE IV

Correlation between the elongation $\Delta R_{\text{O-H}} = R_{\text{O-H}} - R_{\text{O-H}}^g$ of O—H bond length (in Å) of water and the O...H hydrogen bond distance (in Å) of water adsorbed in $\text{Me}^+(\text{H}_2\text{O})$ clusters and in LiABW, NaNAT, BaEDI zeolites relative to the gas state $R_{\text{O-H}}^g$ distances of water obtained with HF and B3LYP as 0.9489 and 0.9719^a Å, respectively.

O...H	HF				B3LYP				
	Me ⁺ (H ₂ O)		Zeolite		O...H	Me ⁺ (H ₂ O)		Zeolite	
	$R_{\text{O-H}}$	$\Delta R_{\text{O-H}}$	$R_{\text{O-H}}$	$\Delta R_{\text{O-H}}$		$R_{\text{O-H}}$	$\Delta R_{\text{O-H}}$	$R_{\text{O-H}}$	$\Delta R_{\text{O-H}}$
2.189	0.958	0.009	0.951	0.002	2.162	0.978	0.006	0.973	0.001
2.280			0.956	0.007	2.246			0.979	0.007
1.925	0.952	0.003	0.959	0.010	1.894	0.973	0.001	0.982	0.011
2.105			0.950	0.001	2.062			0.972	0.000
1.922	—	—	0.955	0.006	1.901	—	—	0.978	0.006
2.056			0.953	0.004	2.032			0.973	0.001
2.098			0.951	0.002	2.078			0.972	0.000
2.142			0.950	0.001	2.115			0.972	0.000

The water/zeolite geometries were first optimized at the PHF level with STO-3G [6] and then scaled at the periodic B3LYP/ps-21G** level (for the cation basis sets, see Table III).

^a B3LYP optimization constrained by experimental H—O—H = 103.9° value [14] (see text).

for isolated H₂O, we also considered a series of single-point calculations for the three water/zeolite systems (Table III).

The minimum total PHF energy for H₂O/BaEDI is precisely obtained at $s = 1.0422$. For H₂O/LiABW and H₂O/NaNAT, the PHF minimum is obtained at $s = 1.05$, which is very close to the H₂O gas state estimation. The optimal scaled O—H bond lengths of H₂O adsorbed in all three zeolite models range from 0.946 to 0.964 Å (Table II). The minimum total PDFT energy corresponds to $s = 1.02, 1.02, \text{ and } 1.03$ for BaEDI, NaNAT, and LiABW, respectively, which is close to the gas state evaluation $s = 1.014$.

Even when applying the above explained s and t scaling of adsorbed H₂O molecule, the differences between the O—H₁ and O—H₂ bond lengths remain similar, 0.019 and 0.008 Å, to the ones optimized by PHF/STO-3G for H₂O/LiABW and H₂O/NaNAT (Table II), respectively, which is in contradiction with the equal O—H distances for H₂O adsorbed in LiABW or LiBIK [7]. To verify or ascertain this difference, potential energy curves along the O_w—H coordinates were computed for all the protons at the PDFT and PHF/ps-21G** levels (example for NaNAT in Fig. 4; the curves are shifted to a common energy zero minimum for clarity). The potential curves correspond to the total energy variations with the O_w—H distance under

fixed coordinates of the framework atoms and H₂O oxygens. The minimum $R_{\text{O-H}}$ of the curves and the bond elongations $\Delta R_{\text{O-H}} = R_{\text{O-H}} - R_{\text{O-H}}^g$ as compared to the O—H bond length $R_{\text{O-H}}^g$ of the isolated gas state molecule are given in Table IV and Figure 4. The optimized $R_{\text{O-H}}^g$ values for isolated H₂O were obtained using the same basis set as the one used in the periodic calculations with both the HF and B3LYP methods. In all cases, the minimum coordinate $R_{\text{O-H}}$ was obtained from parabolic approximation (Fig. 4). The behavior of the $\Delta R_{\text{O-H}}$ presents the most interesting question and we will discuss it just below.

To calculate the reference $R_{\text{O-H}}^g$ value at the B3LYP level, we fixed the H—O—H angle at the experimental value of 103.9° and obtained $R_{\text{O-H}}^g = 0.972$ Å with B3LYP (Fig. 5). The last value was considered in order to keep a consistent picture between the PHF and PDFT results and to overcome the well-known B3LYP drawback for the optimization of the free H₂O molecule, i.e., the small H—O—H angle of 101° and hence a longer O—H bond of 0.975 Å.

In the NaNAT and BaEDI systems, a clear correlation between the O_w—H elongations and O_z...H hydrogen bond lengths is shown at both HF and DFT levels (Fig. 5 and Table IV). The protons in LiABW show larger $\Delta R_{\text{O-H}}$ values as compared to

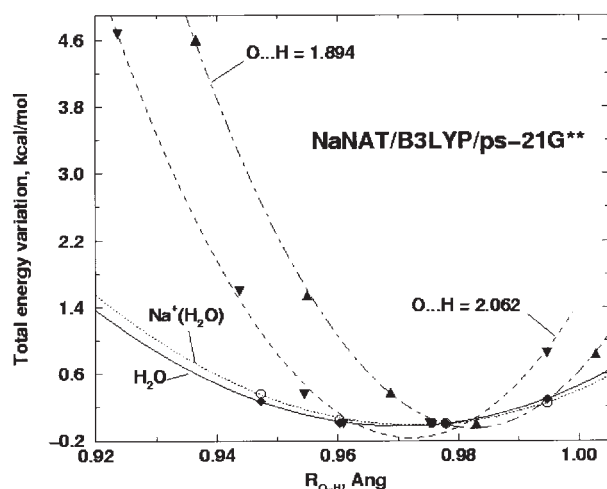


FIGURE 4. Parabolic approximations (lines) of the O_w —H potentials calculated at the B3LYP/ps-21G** level for the isolated water molecule (diamonds), the $Na^+(H_2O)$ cluster (circles), and for both protons of water adsorbed in NaNAT (up and down triangles). Respective lengths of $O_z \dots H$ or $O_w \dots H$ hydrogen bonds (in Å) are given near the lines.

the O—H bonds of the other molecules whose protons are hydrogen bonded at shorter distances in the two other zeolites. These larger ΔR_{O-H} elongations in LiABW can be explained by the influence of the stronger Li coordination to the H_2O oxygen in corroboration to the large ΔR_{O-H} values obtained for the $Li^+(H_2O)$ cluster at both HF (0.009 Å) and B3LYP (0.006 Å) levels (Table IV). The main role of the cation coordination is supported by a higher variation of the Mulliken charge $q(O_w)$ of the H_2O oxygen between $Li^+(H_2O)$ and isolated H_2O , as compared to between $Na^+(H_2O)$ and H_2O . Keeping the same H_2O cluster and H_2O /zeolite geometries, one gets a much larger $q(O_w)$ variation from H_2O to $Me^+(H_2O)$, i.e., by 0.1 and 0.092 e for $Me = Li$, with HF and B3LYP, respectively, as compared to only 0.023 and 0.009 e for $Me = Na$.

The replacement of the O—H lengths in all zeolite models by the values scaled at the PDFT level (given by bold values in Table II) results in lower total energies by 2.31, 3.12, and 3.43 kcal/mol for LiABW, NaNAT, and BaEDI (for the latter, 3.43 corresponds to a scaling of both H_2O molecules in BaEDI), respectively, at the same H—O—H angle as optimized at the first step. Upon these fixed O—H bond lengths, the scaling of the H—O—H angles lowers the energy by 0.44, 0.16, 0.20, and 0.04 kcal/mol for the LiABW, NaNAT, and BaEDI (0.20

and 0.04 corresponds to separate scaling of both H_2O molecules in BaEDI), respectively, as compared to the energy with the angles optimized at the PHF/STO-3G level. The small variations of the H—O—H angles with respect to the PHF/STO-3G values observed upon the angle scaling thus proves the accuracy of the H—O—H angle optimization at the minimal PHF/STO-3G level [5, 6]. The final fractional coordinates of the H_2O atoms are presented in Table V. The initial XRD, optimized, and scaled H_2O geometries are summarized in Table II.

The small perturbation of the H_2O geometry in the adsorbed state as compared to the gas state proves the absence of any specific strong interaction and can thus justify the partial optimization applied herein. The scaling proposed cannot, however, provide the precise adsorbate position at the energy minimum calculated at the B3LYP/ps-21G** level because the energy is not optimized in the full coordinate space at this level. Nevertheless, the small difference between the energy minimum along the “water oxygen–zeolite cation” distance

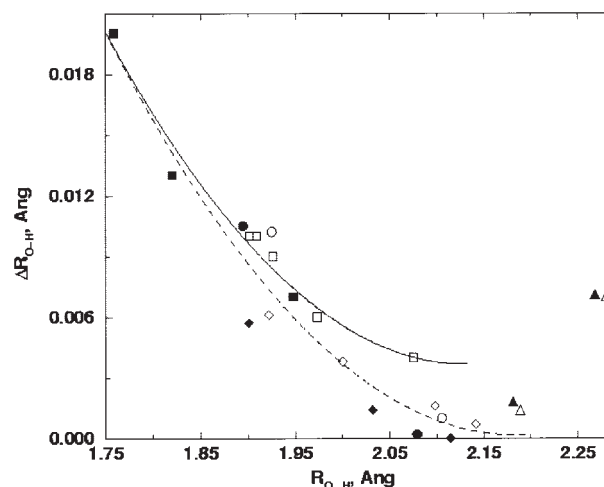


FIGURE 5. Correlation between the elongation of the O—H bond length (ΔR_{O-H} , Å) of water with respect to the gas state and the $O \dots H$ hydrogen bond distance (Å) of water adsorbed in LiABW (triangles), NaNAT (circles), BaEDI (diamonds). Hartree–Fock (HF) and B3LYP results are given by open and closed symbols, respectively. Correlation $\Delta R_{O-H}/O \dots H$ is also given for $(H_2O)_n$ clusters at the HF ($n = 2-6$, open squares) and MP2 ($n = 2-4$, closed squares) levels [8]. Lines correspond to the parabolic approximation of the theoretical data for the $(H_2O)_n$ clusters at both HF and MP2 levels [8] (solid line, $r^2 = 0.987$) and the set of data for the zeolites (with exception of LiABW) and $(H_2O)_n$ clusters (dashed line, $r^2 = 0.93$), respectively.

TABLE V
Optimized fractional atomic coordinates of the oxygens and Li atom in LiABW, of the Na atom in NaNAT, and of water adsorbed in the three cationic zeolite structures.

Zeolite	Atom	X	Y	Z
LiABW	O ₂	0.2718	0.2197	0.1390
<i>a</i> = 10.1023	O ₃	0.1911	0.0399	0.5903
<i>b</i> = 8.1333	O ₄	0.1803	-0.0988	0.0705
<i>c</i> = 4.9509	Li	0.1944	0.6915	0.2556
	H	0.5420	0.1725	-0.1329
	H	0.5125	0.0752	-0.4025
	O _w	0.4738	0.1138	-0.2326
NaNAT	Na	0.2208	0.0316	-0.3821
<i>a</i> = 18.288	H	0.1023	0.1924	0.1803
<i>b</i> = 18.631	H	0.0536	0.1454	0.0354
<i>c</i> = 6.583	O _w	0.0552	0.1906	0.1117
BaEDI	H	0.3714	-0.2406	-0.0574
<i>a</i> = 9.537	H	0.2606	-0.1284	-0.0637
<i>b</i> = 9.651	O _w	0.1718	0.3244	0.1524
<i>c</i> = 6.509	H	0.3011	0.0893	0.0490
	H	0.4142	0.2033	0.0371
	O _w	0.3825	0.1189	-0.0295

Symmetry groups are given in Table I. Other (nonoptimized) coordinates and cell parameters *a*, *b*, *c* (in Å) are from Refs. [9–11] for LiABW, NaNAT, and BaEDI, respectively, with the exception of the cell parameters of LiABW also optimized herein.

upon shifting from PHF/STO-3G to B3LYP/ps-21G** has been proved for BaEDI with single-point calculations. It has been evaluated as 0.019 and 0.006 Å for the two H₂O molecules with respect to the Ba cation. Such minor Me—O_w changes should lead to small variations of the O_w...H distances and do not change the dependences for the H₂O/zeolite represented in Figure 5 even after total optimizations of the systems.

Conclusions

The aim of this work was to study the O—H distortions of H₂O adsorbed in several chosen zeolite models with PHF and PDFT and various basis set levels with CRYSTAL95 [12]. The atomic positions of one crystallographic independent H₂O molecule per elementary unit cell (UC) for the NAT and ABW zeolites, and of the two H₂O molecules for EDI were optimized. Particularly, we proposed a three-step optimization procedure: (1) an initial PHF optimization with the minimal STO-3G basis

set including the positions of the cations in ABW and NAT as well as of some framework atoms in the case of ABW, followed by (2) a distance (*s*) and angle (*t*) scaling of the “isolated whole H₂O molecule” to an upper level of theory and basis sets (conserving the ratios of O—H lengths obtained at the first step), and (3) an optimization of the proton positions in the H₂O/zeolite via systematic variations of each O—H bond length and of the H—O—H angle values at fixed position of the oxygen atom. The last two steps were realized at the B3LYP/ps-21G* level.

The total stabilization energy of the H₂O/zeolite complex is comparable at steps (1) and (2) and with the O—H optimization at step (3), but is rather small with the H—O—H angle scaling of step (3). A clear O_w—H/O_z...H correlation was observed for NaNAT and BaEDI, which resulted in the increase of the O_w—H bond length (up to 0.01 Å) after all three steps. In the case of LiABW, the strong Li cation influence dominates over hydrogen bonding (HB) as confirmed by ab initio computations for the isolated Li⁺(H₂O) cluster at the same basis set level and geometry. The application of the O—H length scaling of the H₂O/zeolite PHF optimized model is thus an appropriate tool to refine the geometry at a higher level basis set. Rather large H—O—H angles, i.e., between 108.2, 107.6, and 105.8°, as compared to the gas state value were observed for all H₂O molecules with the exception of one angle, 101.7°, in BaEDI. The PHF optimization for the H—O—H angles at the minimal basis set level is considered as satisfactory, the errors ranging from 0.8° in the case H₂O/BaEDI to 2.8° for H₂O/LiABW as evaluated at the B3LYP/ps-21G** level.

The O—H elongations ΔR_{O-H} of adsorbed H₂O are small, with a maximum being between 0.010 and 0.006 Å with both PHF or PDFT methods in agreement with more accurate HF and MP2 results for (H₂O)_n clusters. The $\Delta R_{O_w-H/O_z...H}$ correlation has a character similar to the one of $\Delta R_{O_w-H/O_w...H}$ observed in small (H₂O)_n clusters [8].

ACKNOWLEDGMENTS

The calculation were performed on the Interuniversity Scientific Computing Facility (ISCF) Centre installed at the FUNDP, for which the authors acknowledge the financial support of the FNRS-FRFC and the Loterie Nationale for the convention n 2.4578.02. The authors thank Dr. E. Kryachko for fruitful discussions, and the Interuniversity Research Program on “Quantum Size Effects in Nano-

structural Materials" (PAI/IUAP V/01) for partial support.

References

1. Civalleri, B.; D'Arco, Ph.; Orlando, R.; Saunders, V. R.; Dovesi, R. *Chem Phys Lett* 2001, 348, 131.
2. Larin, A. V.; Vercauteren, D. P. *Int J Quant Chem* 2001, 82, 182.
3. Larin, A. V.; Vercauteren, D. P. *Int J Quant Chem* 2001, 83, 70.
4. Larin, A. V.; Vercauteren, D. P. *J Mol Cat A* 2001, 168, 123.
5. Larin, A. V.; Vercauteren, D. P. *Stud Surf Sci Catal* 2001, 135, 263.
6. Larin, A. V.; Trubnikov, D. N.; Vercauteren, D. P. *Int J Quantum Chem* 2003, 92, 71.
7. Fois, E.; Gamba, A.; Tabacchi, G.; Quartieri, S.; Vezzalini, G. *J Phys Chem B* 2001, 105, 3012.
8. Xantheas, S. S.; Dunning, T. H., Jr. *J Chem Phys* 1993, 99, 8774.
9. Krogh Andersen, E.; Ploug-Sorensen, G. *Z Kristallogr* 1986, 176, 67.
10. Ghermani, N. E.; Lecomte, C.; Dusausoy, Y. *Phys Rev B* 1996, 53, 5231.
11. Kwick, Å, Smith, J. V. *J Chem Phys* 1983, 79, 2356.
12. Dovesi, R.; Saunders, V. R.; Roetti, C.; Causà, M.; Harrison, N. M.; Orlando, R.; Aprà, E. *CRYSTAL95 1.0, User's Manual*; Univ. of Torino, 1996.
13. Frisch, M. J.; Trucks, G. W.; Schlegel, H. B.; Scuseria, G. E.; Robb, M. A.; Cheeseman, J. R.; Zakrzewski, V. G.; Montgomery, J. A., Jr.; Stratmann, R. E.; Burant, J. C.; Dapprich, S.; Millam, J. M.; Daniels, A. D.; Kudin, K. N.; Strain, M. C.; Farkas, O.; Tomasi, J.; Barone, V.; Cossi, M.; Cammi, R.; Mennucci, B.; Pomelli, C.; Adamo, C.; Clifford, S.; Ochterski, J.; Petersson, G. A.; Ayala, P. Y.; Cui, Q.; Morokuma, K.; Malick, D. K.; Rabuck, A. D.; Raghavachari, K.; Foresman, J. B.; Cioslowski, J.; Ortiz, J. V.; Baboul, A. G.; Stefanov, B. B.; Liu, G.; Liashenko, A.; Piskorz, P.; Komaromi, I.; Gomperts, R.; Martin, R. L.; Fox, D. J.; Keith, T.; Al-Laham, M. A.; Peng, C. Y.; Nanayakkara, A.; Challacombe, M.; Gill, P. M. W.; Johnson, B.; Chen, W.; Wong, M. W.; Andres, J. L.; Gonzalez, C.; Head-Gordon, M.; Replogle, E. S.; Pople, J. A. *Gaussian 98, Revision A.7*; Gaussian, Inc.: Pittsburgh, PA, 1998.
14. Chase, M. W., Jr.; Davies, C. A.; Downey, J. R., Jr.; Frurip, D. J.; McDonald, R. A.; Syverud, A. N. *JANAF Thermochemical Tables*; *J Phys Chem Ref Data* 14, Suppl 1, 1985.